

Quantitative anatomy of the round window and cochlear aqueduct in guinea pigs

Adam F. Ghiz^a, Alec N. Salt^{a,*}, John E. DeMott^a, Miriam M. Henson^b,
O. William Henson Jr.^c, Sally L. Gewalt^d

^a Department of Otolaryngology, P.O. Box 8115, Washington University School of Medicine, 517 South Euclid Avenue, St. Louis, MO 63110 USA

^b Division of Otolaryngology/Head and Neck Surgery, The University of North Carolina, Chapel Hill, NC 27599 USA

^c Department of Cell Biology and Anatomy, The University of North Carolina, Chapel Hill, NC 27599 USA

^d Center For In Vivo Microscopy, Department of Radiology, Duke University Medical Center, Durham, NC 27710 USA

Received 23 April 2001; accepted 14 August 2001

Abstract

In order to analyze the entry of solutes through the round window membrane, a quantitative description of round window anatomy in relationship to scala tympani is required. High-resolution magnetic resonance microscopy was used to visualize the fluid spaces and tissues of the inner ear in three dimensions in isolated, fixed specimens from guinea pigs. Each specimen was represented as consecutive serial slices, with a voxel size of approximately $25 \mu\text{m}^3$. The round window membrane, and its relationship to the terminal portion of scala tympani in the basal turn, was quantified in six specimens. In each image slice, the round window membrane and scala tympani were identified and segmented. The total surface area of the round window membrane averaged 1.18 mm^2 (S.D. 0.08, $n=6$). The length and variation of cross-sectional area as a function of distance for the cochlear aqueduct was determined in five specimens. The cochlear aqueduct was shown to enter scala tympani at the medial limit of the round window membrane, which corresponded to a distance of approximately 1 mm from the end of the scala when measured along its mid-point. These data are of value in simulating drug and other solute movements in the cochlear fluids and have been incorporated into a public-domain simulation program available at <http://oto.wustl.edu/cochlea/>. © 2001 Elsevier Science B.V. All rights reserved.

Key words: Cochlea; Perilymph; Round window; Scala tympani; Cochlear aqueduct

1. Introduction

The delivery of drugs into the cochlear fluids across the round window membrane is increasingly becoming used in both research experiments and in clinical practice. In humans, direct round window membrane application of gentamicin is now widely used in the treatment of Meniere's disease (Commins and Nedzelski, 1996; Blakley, 1997). Other applications include the administration of steroids or other agents for sudden

hearing loss or autoimmune deafness (Blakley, 1997). Implantable drug delivery systems for therapy to the inner ear have also been developed (Silverstein, 1999; Lehner et al., 1997), including the use of a catheter positioned near the round window membrane such as the μ -Cath, marketed by Durect Inc., Cupertino, CA, USA. In animals, application of drugs and solutes across the round window membrane is being performed for many different experimental situations (Brummett et al., 1976; Zheng et al., 1997; Conlon et al., 1998; Hoffer et al., 1999; Parnes et al., 1999).

Advances in high-resolution magnetic resonance microscopy (MRM) have enabled visualization of the spiral, fluid-filled spaces of the cochlea (Henson et al., 1994; Salt et al., 1995; Wilson et al., 1996). In a previous study (Thorne et al., 1999), lengths, areas, and volumes of the three cochlear scalae were derived for

* Corresponding author. Tel.: +1 (314) 362-7560;
Fax: +1 (314) 362-7522.

E-mail address: salta@msnotes.wustl.edu (A.N. Salt).

Abbreviations: MRM, magnetic resonance microscopy; CSA, cross-sectional area

the cochleae of six species from 3-D reconstructions of high-resolution MRM data sets. These data are of particular value in modeling drug and other solute movements in the cochlear fluids and have been incorporated into a public-domain simulation program (<http://oto.wustl.edu/cochlea/>). The major value of high-resolution MRM data sets is that the true 3-D geometry of the specimen is maintained in a non-destructive technique so that high-resolution MRM is an ideal technique for quantitative analysis of the complex geometry of inner ear structures. MRM data sets are comprised of up to 256 slices, which can be manipulated as required for the data analysis. The possibility of orienting and then digitally reslicing a specimen in a specific plane is an important feature that enables the consistent detailed analysis of specific structures, as required for this study.

In order to determine the actual drug concentrations achieved by round window application, mathematical simulation of solute entry through the round window membrane is required. Such analysis requires an accurate quantitative anatomic description of the structures. It is not adequate to know just the diameter and area of the round window membrane, as has been reported previously (Fernandez, 1952), but rather it is necessary to determine how the 3-D structure of the round window relates to the varying dimensions of scala tympani (ST). A determination of how the area of segments of the round window membrane vary as a function of length along the basal turn of ST enables accurate simulations of solute movement across the round window membrane and into ST perilymph. In addition, to better simulate the role of fluid movements through the cochlear aqueduct on perilymph composition, knowledge of the dimensions of the cochlear aqueduct and where the aqueduct enters ST are required. The anatomy and dimensions of the cochlear aqueduct and how they relate to function has been studied in human temporal bones (Gopen et al., 1997). A morphometric study has also been performed using histologic sections of the inner ear of guinea pigs (Shinomori et al., 2001).

The present study was designed to quantify the 3-D geometry of the round window membrane and the cochlear aqueduct and how the area of each varies as a function of length.

2. Materials and methods

2.1. Tissue preparation

Six pigmented, NIH-strain guinea pigs were utilized in the study. The guinea pigs were anesthetized with a combination of sodium pentobarbital (25 mg/kg given intraperitoneally) and Innovar vet (0.35 ml/kg given intramuscularly). The ears were fixed by whole-head

vascular perfusion using Heidenhain–Susa fixative. While under anesthesia, the ascending aorta was cannulated and the descending aorta was clamped. Approximately 100 ml saline was perfused through the vasculature to wash out the blood. This was followed by perfusion with 200 ml of fixative. The Heidenhain–Susa fixative consists of a stock of solution containing 45 g HgCl₂, 5 g NaCl, 20 g trichloroacetic acid, 40 ml of glacial acetic acid, and 800 ml of distilled water. Immediately prior to use, 240 ml of the stock solution was mixed with 60 ml of 37% formaldehyde. After fixation, the temporal bones were removed, the auditory bullae were opened, and the ears were immersed in fixative for 48 h at 4°C with periodic agitation. After this time, the temporal bones were transferred to 4% phosphate-buffered formaldehyde and stored at room temperature. One guinea pig ear was fixed with 3.1% glutaraldehyde in phosphate-buffered Hank's balanced salt solution, and after 6 days was post-treated for 24 h with solution containing HgCl₂ at 10% of the concentration in Heidenhain–Susa. In these procedures, treatment with HgCl₂ was necessary to enhance the contrast of the membranous structures, including the round window and Reissner's membranes, making them appear black against the light fluid spaces.

2.2. Magnetic resonance imaging

After fixation, the temporal bones were carefully trimmed until the cochlear portion would fit into a cubic space with 6.4 mm on each side. Approximately 24 h prior to scanning, the specimen was placed in solution containing Magnevist (a commercially available contrast agent; Berlex Laboratories, Wayne, NJ, USA; dilution of 1:500). MRM was performed at the Center for In Vivo Microscopy at Duke University, Raleigh, NC, USA. The MRM system was a GE Omega System with a 7.1 T, 15-cm-diameter horizontal bore superconducting magnet, with 85 gauss/cm shielded gradients. The radiofrequency coil was a Helmholtz pair, 15 mm in diameter and with variable separation, as specially designed for imaging small specimens (Banson et al., 1992). Cochleae were placed within the well of a 6-mm-thick plexiglass slide (5×1.5 cm) which was custom-made to fit into a small radiofrequency coil. The well was filled with fluid containing contrast agent. The acquisition parameters were: 13.5 h acquisition time, 6.5 ms echo time, 375 ms repetition time, 2 excitations, and 6.4 mm field of view in each dimension. The acquisition array size was 256×256×256, generating cubic voxels 25 μm on each side.

2.3. Analysis

The segmentation and reconstruction of the fluid

spaces (base of ST and cochlear aqueduct) and the round window membrane utilized methods that have been documented previously (Salt et al., 1995; Wilson et al., 1996). Analysis of MRM images was performed using the public-domain program NIH Image (written by Wayne Rasband at the NIH and available on the Internet at <http://rsb.info.nih.gov/nih-image/>) on a Power Macintosh 6400. Specific spaces and structures were segmented from the original gray-scale image stack, using suitable density thresholds to allow outlining of the structure or space. In cases where boundaries could not be automatically selected, they were defined by the investigator. Outlined structures were colored white in each image slice, following which the entire stack was converted to a binary form to simplify further analysis. The binary stack representing the 3-D structure maintained registry with the original data set. Determining the cross-sectional areas (CSA) of fluid-filled spaces has previously been performed using custom macros for NIH image that section the binary volumes in arbitrary planes until a section is obtained orthogonally to the long axis of the scala (Salt et al., 1995). Using this automated algorithm, it was apparent that the basal 2–3 mm of ST could be closely approximated as a straight tube. An axis was therefore defined along

the mid-point of ST that was extended through the region of the round window. The specimen was subsequently rotated and resliced with the plane of sectioning orthogonal to this defined long axis of the scala. Each resulting slice showed segments of ST and round window, from which the CSA of both were determined in each segment by voxel counts.

CSA and length measurements of five cochlear aqueducts of five specimens were determined using a custom macro as previously detailed (Salt et al., 1995). An additional macro had been written previously (Thorne et al., 1999) to derive the total fluid space volume from the total voxel count, with each voxel representing a volume of 15.62 pl.

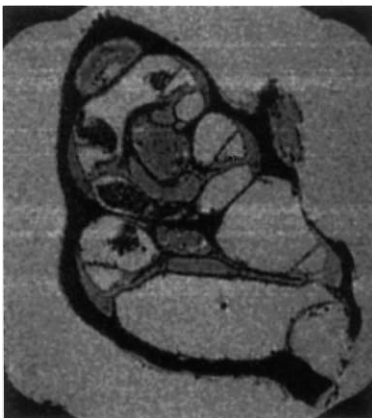
The care and use of guinea pigs in this study were approved by the Animal Studies Committee of Washington University, St. Louis, MO, USA (approval numbers 91062 and 95069).

3. Results

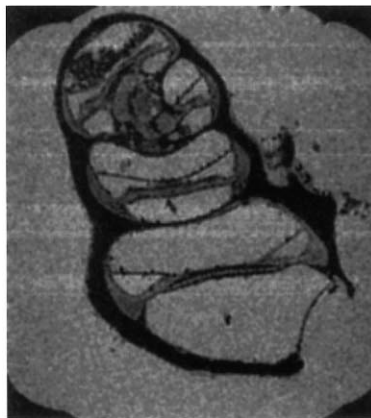
An initial analysis of round window membrane area was performed by segmenting the round window membrane from the original gray-scale image stack. Fig. 1

Raw Data

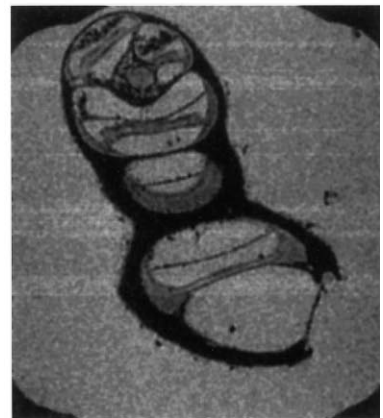
Slice 105 / 183



Slice 123 / 183



Slice 138 / 183



Round Window Membrane Segmented

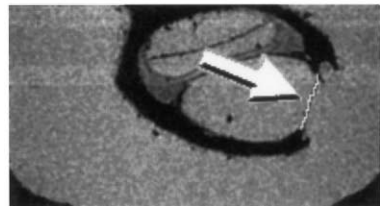
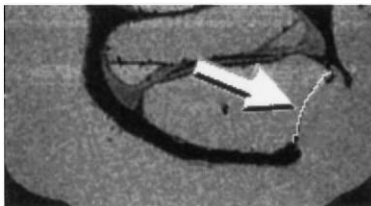
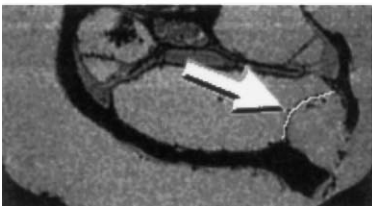


Fig. 1. Three representative sections of the 3-D image stack showing the relationship of the round window to ST in the guinea pig. The specimen has been orientated so that the round window is orthogonal to the section. Each specimen is also shown with the round window membrane identified and segmented, as shown in white.

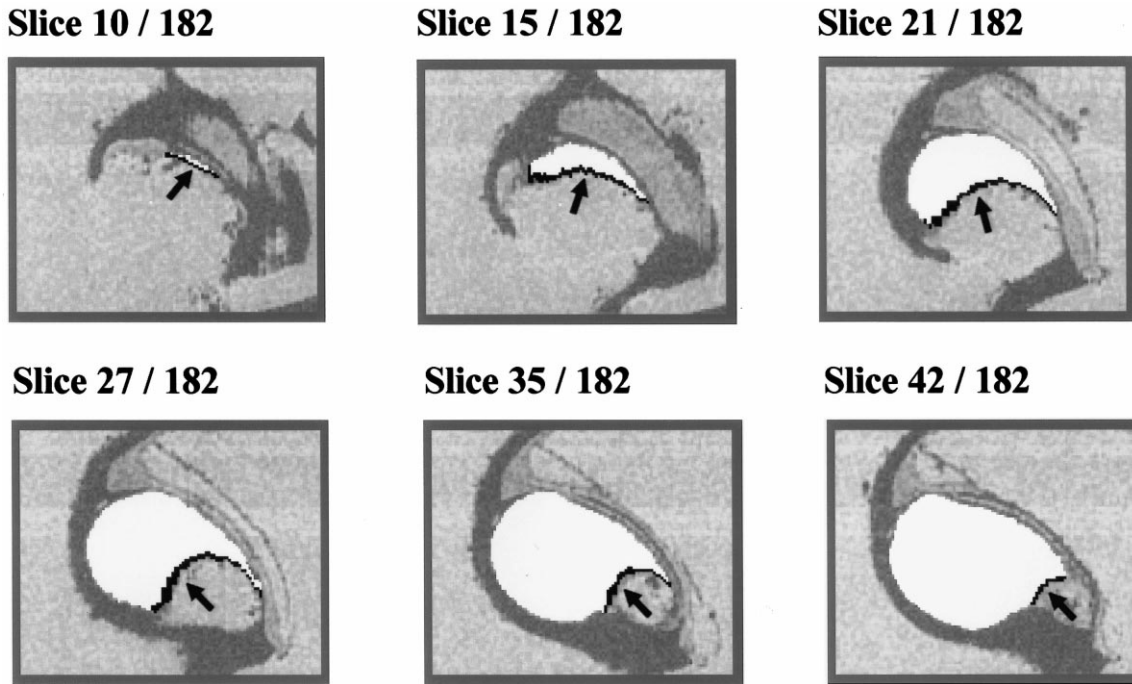


Fig. 2. The same specimen as Fig. 1 which has been oriented with the plane of sectioning orthogonal to the longitudinal axis of ST. The example sections show six of the approximate 40 slices in which the round window membrane is visible (shown black and the middle ear surface indicated by an arrow). The slice number is indicated in each case. The corresponding CSA of ST is segmented white. The remaining specimen is shown in low contrast. Slice 10 is close to the limit of the round window at the limit of the scala (upper left). Slice 42 shows a section of the round window at the greatest distance from the end of the scala (lower right). In some sections (slice 27) the round window is more than one voxel wide in some regions due to the tangential plane of sectioning with this orientation.

shows the data set of one specimen oriented so that the round window (delineated by the arrow) was orthogonal to the plane of slicing. The round window surface in each slice was segmented by the investigator, and is shown as white in the figure. The surface area of the round window segment in each section was quantified for each slice of the specimen in which it was visible. This was determined by analyzing the line fitted through the membrane using the 'perimeter measurement' algorithm, a routine that takes the geometry of voxels into account. Half of the perimeter value, which corresponds to one surface of the membrane, multiplied by the voxel width, gave the round window area in that section. The area values for each section were then summed to obtain a total surface area for each specimen. The mean round window area for the guinea pig determined for six specimens by this method was 1.18 mm^2 (S.D. 0.08).

The relationship of the round window to ST was established using specimens oriented so that the plane of sectioning was orthogonal to the long axis of ST, as shown in Fig. 2. Each resulting slice contained a segmented portion of ST (shown white) in contact with a corresponding segment of the round window membrane (shown black). Voxel counts of both ST and the round window were performed for each section. The CSA of ST was derived using an area of $6.25 \times 10^{-4} \text{ mm}^2/\text{voxel}$.

Due to the fact that the round window was in some areas sectioned obliquely in this orientation, the area assigned to each section was determined as the proportion of the total round window area based on the number of round window voxels found in the segment relative to the total count summed across all segments. The findings derived from an analysis of six specimens in this manner are summarized in Fig. 3. The upper part of the figure shows the mean CSA of the ST in the basal turn derived from six specimens. The lower part of Fig. 3 shows corresponding areas of the round window membrane segments in contact with each segment of ST of the same specimen. These data define the area versus distance relationship between the round window membrane and perilymphatic fluid space of ST. One notable feature of the relationship is that much of the area of the round window is associated with the terminal region of ST where the CSA is relatively narrow. This finding is highly relevant to our understanding of drug movements across the structure as this relationship may limit the ability of the solutes to diffuse into the wider regions of ST more distant from the round window. It is also apparent that the highest variability between specimens was associated with the terminal region, probably resulting from differences in the resting position of the membrane in different specimens.

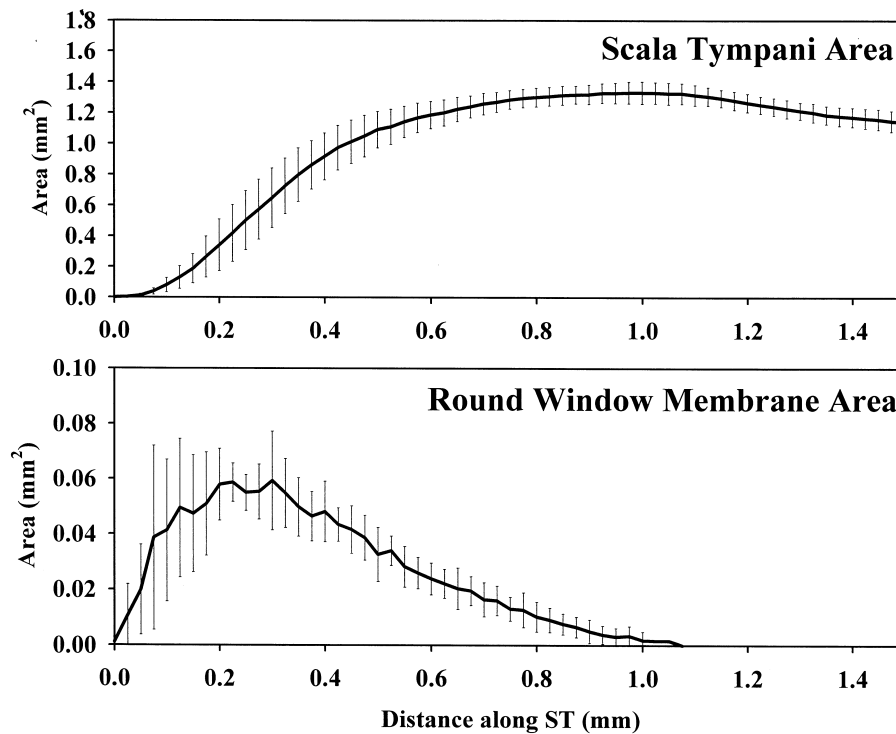


Fig. 3. Summary of the CSA of ST in the basal region of the cochlea (upper panel) and the area of the round window membrane in contact with each corresponding ST fluid segment averaged for six specimens. Bars indicate standard deviation. Note that a considerable proportion of the round window area contacts the terminal portion of ST where CSA is small.

Three views of the 3-D geometric relationships between the round window, the ST, and the cochlear aqueduct are illustrated in Fig. 4. An important consideration is the definition of the terminal region or 'end' of ST. In our analysis, the terminal limit of the scala is not, as commonly believed, at the 'hook' region of the basilar membrane which lies on the medial side of the scala. Rather, the limit represents the lateral portion of the scala, corresponding to the tympanic lip of the round window. Thus, in Fig. 3, it is apparent that the narrowing of ST at the end of the basal turn results

from the angle of the round window membrane, in which the medial portion extends along the scala as it widens from the terminal region. Furthermore, it is clear in Fig. 4 that the ostium where the cochlear aqueduct joins ST is not at the terminal limit of the scala, but is rather at the medial limit of the round window, which corresponds to a distance of 1 mm from the tip of the scala.

To measure the volume and area relationships of the cochlear aqueduct, similar techniques were employed. The cochlear aqueduct was once again segmented as

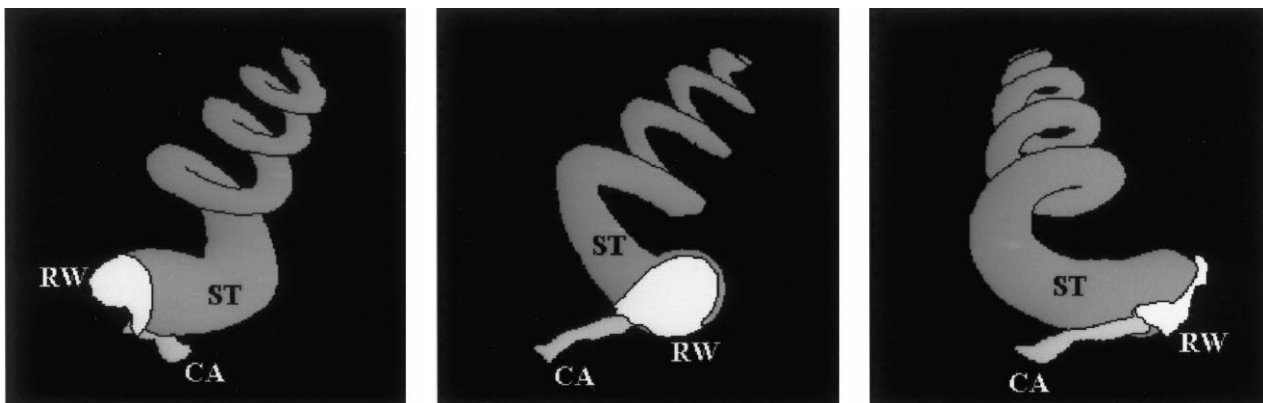


Fig. 4. 3-D rendition of ST (gray) with the round window membrane (RW: white) and the cochlear aqueduct (CA: light gray) showing the geometric relationships. The cochlear aqueduct runs at a shallow angle to ST, joining the scala at the margin of the round window membrane that is approximately 1 mm from the end.

shown in Fig. 4 where the cochlear aqueduct is seen to join ST at some distance from the tip of the scala. One can see that the aqueduct follows a path at a shallow angle to the terminal region of ST until it connects with the sub-arachnoid space. The CSA and length measurements of five cochlear aqueducts of five specimens were determined using the custom macro that followed the mid-point of the tubular structure (Salt et al., 1995), as shown in Fig. 5. The reference point for distance measurements was the point at which the aqueduct joined ST. The area of the duct is lowest as it approaches ST and widens dramatically as it approaches the sub-arachnoid space. The average length of the cochlear aqueduct was measured to be approximately 2 mm ($n = 5$), but an exact measure was not possible because the junction between cochlear aqueduct and sub-arachnoid space is not well delineated. Based on the area–distance relationship shown, the volume of the aqueduct would be 0.08, 0.11 or 0.14 μl if the aqueduct is taken as terminating at 2.0, 2.1 or 2.2 mm, respectively. Thus, volume alone, without documenting the area–distance relationship, is of limited value unless the limit of the aqueduct is carefully defined.

4. Discussion

High-resolution MRM has become an effective tool for imaging the complex 3-D structures of the inner ear, generating images in a form that permits detailed quantitative analysis. Based on these data sets, the relation-

ship of the round window membrane to the terminal region of ST in the basal turn has been more closely defined. In addition, the geometry of the cochlear aqueduct has also been determined.

Fernandez (1952) had previously quantified the round window area of the guinea pig cochlea to be 1.02 mm^2 . This figure was based on the assumption that the round window was elliptical in shape, and was derived by measures of the long and short axes of the ellipse. In our study, we found the area (mean 1.18 mm^2) to be slightly larger than that reported by Fernandez. To determine how much of this difference was caused by Fernandez' assumption of an elliptical round window, with no consideration of the membrane curvature, we too quantified the round window assuming an elliptical shape based on our measures of the vertical and horizontal axes. The area computed in this manner for our specimens was 1.09 mm^2 (S.D. 0.13, $n = 6$), which is quite comparable to Fernandez' study. We can conclude that a failure to consider to curvature of the round window membrane results in a small (approximately 8%) underestimation of the actual area.

The data relating the CSA of the round window membrane to that of the ST are also of considerable value. They show that the round window is not simply an oval at the flat end of a tube. As can be seen in Figs. 3 and 4, the round window membrane extends a little over 1.0 mm from the terminal limit of ST, with the largest area between 0.2 and 0.3 mm from the end. These measures provide a foundation for the calcula-

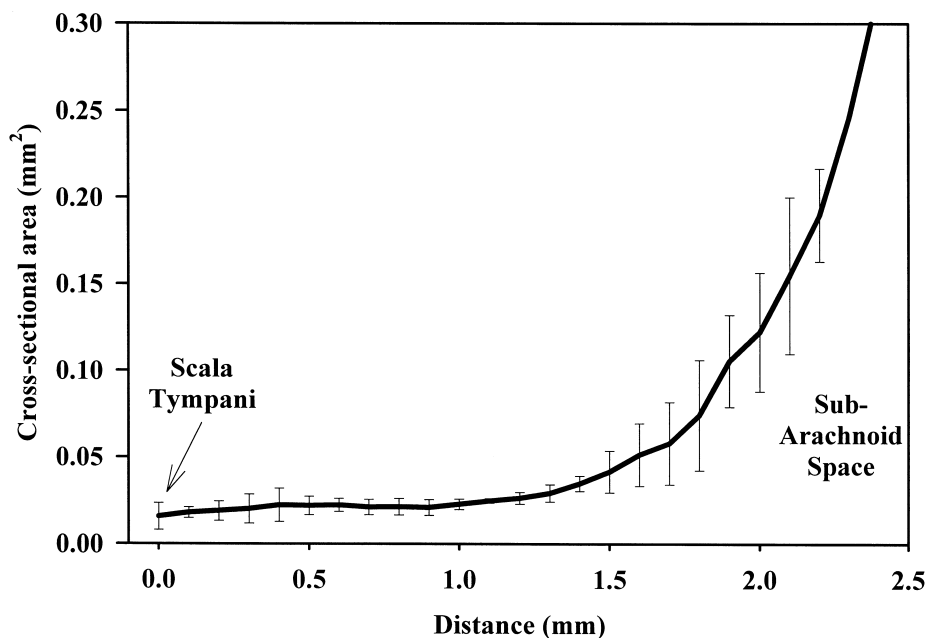


Fig. 5. Summary of the CSA of the cochlear aqueduct as a function of distance from the point where it joins ST for five specimens. Bars indicate standard deviation.

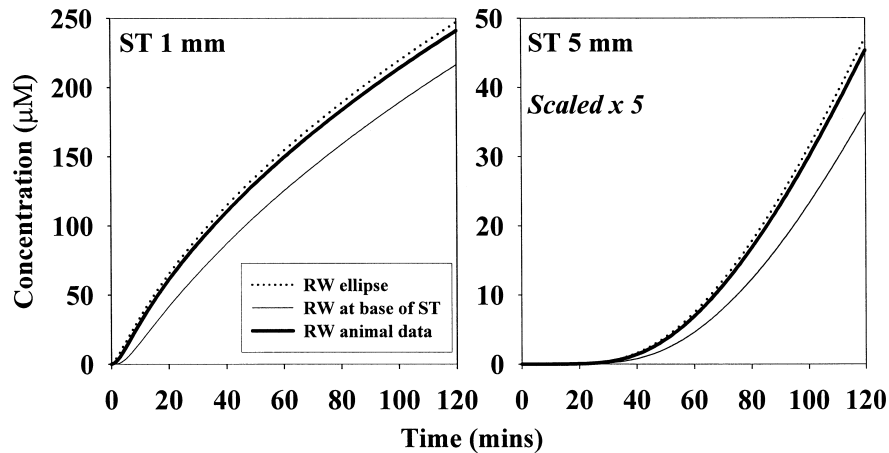


Fig. 6. Calculated influence of round window anatomy data on simulations of solute entry into the cochlea. The curves show three conditions; the round window (RW) simulated as an ellipse extending 1.1 mm from the base of ST (dotted); the RW as the specified area applied to the base of ST (thin line); the RW area distribution and projection along ST established by the data collected in this paper. Solute entry is based on an applied concentration of 1 mM to the round window and is calculated for two locations along ST, 1 mm (ST 1 mm) and 5 mm (ST 5 mm) from the basal end.

tion of the diffusion of drugs and solutes through the round window membrane and into the perilymph of the basal turn of ST. The data have been incorporated into our cochlear fluids simulation program that is used for the design and interpretation of experiments. The simulator was developed and written by Alec Salt and has been made publicly available on the Internet at <http://oto.wustl.edu/cochlea/>. The findings concerning the geometry of the cochlear aqueduct will also enable simulation of interactions occurring between the cerebrospinal fluid in the sub-arachnoid space and the cochlear fluids of the inner ear. Demonstration of the quantitative influences of the data derived from the present analysis on calculated findings are summarized in Fig. 6. In the example shown, the application of a solute with a diffusion coefficient of $0.65 \times 10^{-9} \text{ m}^2/\text{s}$ (comparable to gentamicin) to the round window at an arbitrary concentration of 1 mM has been simulated. Solute entry is calculated for a round window permeability value of $0.1 \times 10^{-9} \text{ m/s}$ and concentration time courses are shown for ST perilymph at sites 1 mm and 5 mm from the basal limit of the scala, with distances measured along the mid-point of the scala. No solute clearance was incorporated into these calculations. Entry is shown for three different implementations of the round window in the model, including that based on the data obtained in this study (heavy line). For comparison, the round window has also been modeled as a simple ellipse having an identical area to that measured for the animal (1.18 mm^2) and extending an identical distance along ST (1.1 mm). This allows the specific influence of the documented round window area as a function of distance to be assessed. Also shown is the calculated entry for the round window implemented as an identical area at the terminal region of ST. For this latter

simulation, the end of ST was modified slightly so that the area of the scala was no smaller than that of the round window. This permitted the influence of the orientation of the round window with respect to ST to be assessed. The curves show that both the round window area data and the orientation with respect to ST influence the calculated concentration profiles. Even excluding the initial period, calculated concentration differences of up to 30% can occur depending on how the round window is modeled. This calculation confirms the necessity of accurate anatomic data for accurate simulations of solute entry into the perilymphatic space.

The anatomic data generated by the present study have already been used in the interpretation of physiologic experiments in which the rate of solute entry across the round window was quantified (Salt and Ma, 2001). Marker was applied in the form of a dilute solution that was continuously irrigated across the round window membrane. Based on the time courses of a marker solute measured by ion-selective electrodes sealed into the first and second turns of ST, we were able to estimate the permeability of the round window, the rate of longitudinal flow in ST, and the rate of solute clearance from ST. Such studies provide a scientific basis for our understanding of drug and other solute movements in the inner ear fluids.

The cochlear aqueduct data reported here compares very well with that reported recently based on 3-D reconstruction of histologic material (Shinomori et al., 2001). In that study, the volume of the cochlear aqueduct was estimated to be 0.113 mm^3 , which is close to the volume we observed. The additional documentation of CSA with distance for the cochlear aqueduct in the present study is of value for the simulation of fluid

interactions between perilymph in ST and the cerebrospinal fluid in the sub-arachnoid space.

Our measurements were made in isolated, fixed specimens and are therefore only an approximation of the actual state in vivo. The dimensions of ST are unlikely to be influenced by fixation, since no decalcification of the otic capsule is necessary for MRM. However, the position of the round window membrane could well be somewhat different in the live specimen, and is likely to vary according to pressure differences between perilymph and the middle ear cavity. Small changes in perilymphatic volume in the basal region are undoubtedly associated with such round window membrane movements. Such factors would be expected to have only a minor influence on solute entry into ST.

Acknowledgements

This work was supported by NIH Grants T32 DC00022 (A.G.), RO1 DC01368 (A.S.), and RO1 DC00114 (O.W.H.). MRM was performed at the Center for In Vivo Microscopy, Department of Radiology, Duke University Medical Center, supported by NIH Grant P41 RR05959.

References

- Banson, M.L., Cofer, G.P., Black, R., Johnson, G.A., 1992. A probe for specimen magnetic resonance microscopy. *Invest. Radiol.* 27, 157–164.
- Blakley, B.W., 1997. Clinical forum: A review of intratympanic therapy. *Am. J. Otol.* 18, 520–526.
- Brummett, R.E., Harris, R.F., Lindgren, J.A., 1976. Detection of ototoxicity from drugs applied topically to the middle ear space. *Laryngoscope* 86, 1177–1187.
- Commins, D.J., Nedzelski, J.M., 1996. Topical drugs in the treatment of Meniere's disease. *Curr. Opin. Otolaryngol. Head Neck Surg.* 4, 319–324.
- Conlon, B.J., McSwain, S.D., Smith, D.W., 1998. Topical gentamicin and ethacrynic acid: effects on cochlear function. *Laryngoscope* 108, 1087–1089.
- Fernandez, C., 1952. Dimensions of the cochlea (guinea pig). *J. Acoust. Soc. Am.* 24, 521–523.
- Gopen, Q., Rosowski, J.J., Merchant, S.N., 1997. Anatomy of the normal human cochlear aqueduct with functional implications. *Hear. Res.* 107, 9–22.
- Henson, M.M., Henson, O.W., Jr., Gewalt, S.L., Wilson, J.L., Johnson, G.A., 1994. Imaging the cochlea by magnetic resonance microscopy. *Hear. Res.* 75, 75–80.
- Hoffer, M.E., Balough, B.J., Kopke, R.D., Henderson, J., DeCiccio, M., Wester, D.C., O'Leary, M.J., Balaban, C., 1999. Morphologic changes in the inner ear of chinchilla laniger after middle ear administration of gentamicin in a sustained-release vehicle. *Otolaryngol. Head Neck Surg.* 120, 643–648.
- Lehner, R., Brugger, H., Maassen, M.M., Zenner, H.P., 1997. A totally implantable drug delivery system for local therapy of the middle and inner ear. *Ear Nose Throat J.* 76, 567–570.
- Parnes, L.S., Sun, A.H., Freeman, D.J., 1999. Corticosteroid pharmacokinetics in the inner ear fluids: An animal study followed by clinical application. *Laryngoscope* 109 (Suppl.), 1–17.
- Salt, A.N., Henson, M.M., Gewalt, S.L., Keating, A.W., Demott, J.E., Henson, O.W., Jr., 1995. Detection and quantification of endolymphatic hydrops in the guinea pig cochlea by magnetic resonance microscopy. *Hear. Res.* 88, 79–86.
- Salt, A.N., Ma, Y., 2001. Quantification of solute entry into cochlear perilymph through the round window membrane. *Hear. Res.* 154, 88–97.
- Shinomori, Y., Spack, D., Jones, D., Kimura, R.S., 2001. Volumetric and dimensional analysis of the guinea pig inner ear. *Ann. Otol. Rhinol. Laryngol.* 110, 91–98.
- Silverstein, H., 1999. Use of a new device, the Microwick, to deliver medication to the inner ear. *Ear Nose Throat J.* 78, 595–598.
- Thorne, M., Salt, A.N., DeMott, J.E., Henson, M.M., Henson, O.W., Gewalt, S.L., 1999. Cochlear fluid space dimensions for six species derived from reconstructions of three-dimensional magnetic resonance images. *Laryngoscope* 109, 1661–1668.
- Wilson, J.L., Henson, M.M., Gewalt, S.L., Keating, A.W., Henson, O.W., Jr., 1996. Reconstructions and cross-sectional area measurements from magnetic resonance microscopic images of the cochlea. *Am. J. Otol.* 17, 347–353.
- Zheng, X.Y., Henderson, D., Hu, B.H., McFadden, S.L., 1997. Recovery of structure and function of inner ear afferent synapses following kainic acid excitotoxicity. *Hear. Res.* 105, 65–76.